A Comparative Study of Extended Kalman Filtering and Unscented Kalman Filtering on Lie Group for Stewart Platform State Estimation

Binhai Xie[1,2,*] and Shuling Dai[1,2,†]
1. State key Laboratory of Virtual Reality Technology and Systems, Beihang University, 100191, Beijing, China;
2. Jiangxi Research Institute, Beihang University(BUAA),100191, Beijing, China;
* e-mail: xiebinhai@buaa.edu.cn
†email: sldai@buaa.edu.cn

2021 6th International Conference on Control and Robotics Engineering (ICCRE) | 978-1-6654-1239-1/20/$31.00 ©2021 IEEE | DOI: 10.1109/ICCRE51898.2021.9435722

***Abstract*—For Stewart platform, high-quality kinematic motion signal plays an vital role in assessing flight training fidelity and providing feedback for trajectory following. In addition to relying on numerically solving forward kinematic problem from measurement of six leg displacement sensors to obtain kinematic motion, some researchers began to employ sensor fusion scheme through deploying inertial measurement unit (IMU) on upper moving platform. In this paper, we will construct Extended Kalman Filtering (EKF) and Unscented Kalman Filtering (UKF) on Lie group to address this fusion problem. This fusion problem is slightly different from Simultaneous Localization and Mapping (SLAM) or Visual Inertial Odometry (VIO) in that six linear displacement sensors are tightly coupled with IMU sensors while those sensors in SLAM or VIO problem still provides partial measurement of motion state. Numerical simulation experiment shows that both Lie group-based EKF (EKF-LG) and UKF (UKF-LG) which satisfy group affine property behave better than conventional Kalman filtering in consistency and accuracy.**

Keywords—Lie group, extended Kalman filtering, unscented Kalman filtering, Stewart platform, sensor fusion

I. INTRODUCTION

For Stewart platform type flight simulator, high-qualty kinematic state around pilot's head is essential to objectively assess its motion cueing fidelity. In [1], Poll proposed a multi-sensor fusion scheme for flight fidelity evaluation. Meanwhile, real-time kinematic state feedback signals are required in design of advanced multi-level controller as stressed in [2]. However, numerical iterative forward kinematic solving algorithms that merely relied on six linear displacement sensors to infer motion state are not longer reliable as they are sensitive to kinematic model accuracy and sensor noise. In addition, velocity and acceleration signals are also needed to be inferred while direct numerical differentiation of calculated position and orientation angles will amplify sensor noise.

In view of all these challenges, some researchers resorted to sensor fusion of IMU sensor mounted on moving platform with six available displacement sensors to reconstruct kinematic state, such as SIMONA flight simulator at Delft University of Technology. An EKF-based 3-DoFs state estimation algorithm was evaluated in [3] for only symmetrical simulator motion. In [4] and [5], Miletović had tried Iterated Extended Kalman Filter (IEKF) and UKF to deal with sensor fusion problem. The idea of using a Kalman filter-based kinematic state estimation algorithm to address sensor fusion problem of inertial sensor with other sensors had been widely demonstrated in robotics, aerospace, etc. These well-known Kalman filter-based algorithms are commonly designed using sensor model that evolves on flat Euclidean space. They assumes state uncertainty with Gaussian distribution on Euclidean space. However, this conventional assumption is not longer valid for nonlinear system model that naturally lives on a manifold. A large class of system models evolved on a Lie group-structured manifold, such as 2D SLAM on SE(2) and aided inertial navigation systems (INS) on SE(3).

Chirikjian [6] and Barfoot [7] began to define state uncertainty using Gaussian distribution in Lie algebra with exponential map. [8] developed a continuous-discrete EFK on matrix Lie group with this assumption. In [9], Bonnable and Barrau introduced an invariant EKF (InEKF) and completed the theory of InEKF with important log-linear property as well as convergence proof. It had been applied to visual inertial navigation system with improved consistency. In [10], Martin made an extension of UKF to models on Lie group. Martin also discussed how symmetry structure in SLAM model affects design of a consistent InEKF algorithm [11]. However, this symmetry structure didn't always exist in multi-sensor fusion model. For example, sensor fusion problem of Stewart platform behaves that the choice of state representation had no impact on observability analysis.

In this paper, we intend to develop Kalman filter-based algorithms on Lie group for Stewart platform state reconstruction in order to achieve robust and consistent properties. The rest of this paper is organized as follows. Section II provides IMU sensor dynamic model and kinematic model of a general Stewart platform. In Section III, we construct two Lie group-based Kalman filtering algorithms (EKF-LG and UKF-LG) and discuss how group structure can affect their filtering performance. A numerical simulation evaluation comparison of these two algorithms with conventional Kalman filtering (UKF-Conv) is carried out in Section IV.

II. Stewart Platform Kinematics and IMU Sensor Dynamics

A. Kinematic Model of Stewart Platform

A geometric structure of Stewart platform is depicted in Fig. 1.

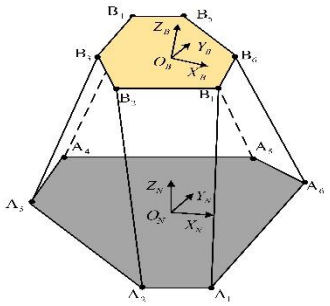

Fig. 1. Geometric structure of Stewart platform

Two coordinate frames $\{N-X_NY_NZ_N\}$ and $\{B-X_BY_BZ_B\}$ are fixed at lower and upper platform with their orgins O_N and O_B fixed at geometric center of each platform. Orientation matrix R denotes transformation from moving frame {B} to fixed inertial frame {N}. Let p and v be position and velocity vector of center O_B represented in frame {N}. The kinematic state of moving platform to be estimated can be packed into state $\chi \in SE_2(3)$.

$$\chi = \begin{bmatrix} R & v & p \\ 0_{1\times 3} & 1 & 0 \\ 0_{1\times 3} & 0 & 1 \end{bmatrix} \in SE_2(3) \tag{1}$$

Inverse kinematic of this platform refers to a mapping from moving platform pose (R, p) to six leg lengths. Each leg length can be expressed in Euclidean norm as follows,

$$l_i = h_i(\chi) = \left\| Rb_i + p - a_i \right\|_2, i = 1,\cdots,6 \tag{2}$$

where b_i is coordinate vector for i-th upper joint center B_i in frame {B} and a_i is coordinate vector for i-th lower joint center A_i in frame {N}. All leg lengths are formulated into a six-dimensional vector function $h(\chi) = [h_1,\cdots,h_6]^T$.

Let $h(\exp(\xi)\circ\chi)$ denotes small incremental change along right version of Lie algebra vector ξ. After applying first order approximation to exponential map and Taylor series expansion of Euclidean norm $\|b+\delta\| \approx \|b\| + b^T\delta/\|b\|$ to (2), we can approximate function $h(\chi)$ around χ in the following equation.

$$h(\exp(\xi)\circ\chi) = h(\chi) + H\xi + \mathcal{O}\left(\|\xi\|^2\right) \tag{3}$$

where Jacobian matrix H is given as follows,

$$H = \begin{bmatrix} \frac{1}{l_1}\left(a_1 \times (Rb_1 + p)\right)^T & 0_{1\times 3} & \frac{1}{l_1}(Rb_1 + p - a_1)^T \\ \vdots & \vdots & \vdots \\ \frac{1}{l_6}\left(a_6 \times (Rb_6 + p)\right)^T & 0_{1\times 3} & \frac{1}{l_6}(Rb_6 + p - a_6)^T \end{bmatrix} \tag{4}$$

B. IMU Sensor Dynamic Model

As IMU sensor is assumed to be mounted at geometric center of upper platform, its kinematic state herein equals to kinematic state of upper platform. Generally, IMU sensor output data are commonly biased and highly noisy as follows,

$$\begin{aligned} \omega_m &= \omega + b_g + n_g, n_g \sim \mathcal{N}\left(0_{3\times 1}, \Sigma^g\right) \\ a_m &= a + b_a + n_a, n_a \sim \mathcal{N}\left(0_{3\times 1}, \Sigma^a\right) \end{aligned} \tag{5}$$

where b_g and b_a are biases of gyro and accelerometer respectively. n_g and n_a are white Gaussian distribution vectors.

As IMU sensor is fusing with six displacement sensors, its drift effect is expected to be reduced by including its bias vector $b \triangleq (b_g, b_a)$ into state to be estimated. Hence $\chi_{\mathcal{L}} \triangleq (\chi, b)$ belongs to an augmented state space $\mathcal{L} = SE_2(3)\times\mathbb{R}^3\times\mathbb{R}^3$.

$$\chi_{\mathcal{L}} = \left[\begin{array}{ccc:cc:cc} R & v & p & & & & \\ 0_{1\times 3} & 1 & 0 & \multicolumn{2}{c:}{0} & \multicolumn{2}{c}{0} \\ 0_{1\times 3} & 0 & 1 & & & & \\ \hdashline \multicolumn{3}{c:}{\multirow{2}{*}{0}} & I_3 & b_g & \multicolumn{2}{c}{\multirow{2}{*}{0}} \\ \multicolumn{3}{c:}{} & 0_{1\times 3} & 1 & \multicolumn{2}{c}{} \\ \hdashline \multicolumn{3}{c:}{\multirow{2}{*}{0}} & \multicolumn{2}{c:}{\multirow{2}{*}{0}} & I_3 & b_a \\ \multicolumn{3}{c:}{} & \multicolumn{2}{c:}{} & 0_{1\times 3} & 1 \end{array}\right] \triangleq \begin{bmatrix} R \\ v \\ p \\ b_g \\ b_a \end{bmatrix}_{\mathcal{L}} \tag{6}$$

With these assumptions, a continuous stochastic IMU dynamics can be expressed in form of $\chi_{\mathcal{L}}$ using following differential equation. Let $u = \left[a_m^T, \omega_m^T\right]^T$ denotes input to IMU model.

$$\frac{d}{dt}\chi_{\mathcal{L}} = f_u(\chi_{\mathcal{L}}) - \chi_{\mathcal{L}} n_t^{\wedge} \tag{7}$$

where,

$$f_u(\chi_{\mathcal{L}}) = \begin{bmatrix} R(\omega_m - b_g)_\times \\ R(a_m - b_a) + g \\ v \\ 0_{3\times 1} \\ 0_{3\times 1} \end{bmatrix}_{\mathcal{L}}, n_t^{\wedge} = \begin{bmatrix} (n_g)_\times \\ n_a \\ 0_{3\times 1} \\ n_{b_g} \\ n_{b_a} \end{bmatrix}_{\mathcal{L}} \tag{8}$$

where $f_u(\bullet)$ denotes unnoisy deterministic dynamic model and noise vector $n_t \triangleq \left(n_g, n_a, 0_{3\times 1}, n_{b_g}, n_{b_a}\right)$ consists of all these four kinds of noises. $(\bullet)^{\wedge}: \mathbb{R}^{\dim \mathfrak{g}} \to \mathfrak{g}$ denotes a linear isomorphism from vector space to Lie algebra. $(\bullet)_\times$ denotes 3×3 skew symmetric operator and g is constant gravity vector. Both gyro and accelerometer biases are modeled as random walks driven by white Guassian noise n_{b_g} and n_{b_a}.

It is verified that $f_u(\bullet)$ satisfies group affine property, i.e. $f_u(\chi_1\cdot\chi_2) = f_u(\chi_1)\chi_2 + \chi_1 f_u(\chi_2) - \chi_1 f_u(I_d)\chi_2$ for all $\chi_1, \chi_2 \in \mathcal{L}$. With this property, an error model based on right invariant error η (i.e. $\eta = \bar{\chi}_{\mathcal{L}} \cdot \chi_{\mathcal{L}}^{-1}$) can be derived.

$$\frac{d}{dt}\xi_{\mathcal{L}} = A\cdot\xi_{\mathcal{L}} + \begin{bmatrix} Ad_{\chi} & 0_{9\times 6} \\ 0_{6\times 9} & I_6 \end{bmatrix}\cdot n_t \tag{9}$$

where Ad_{χ} denotes adjoint matrix of state χ and A donotes Jacobian matrix with respect to Lie algebra vector $\xi_{\mathcal{L}}$ in following explicit formulations.

$$A = \begin{bmatrix} 0_3 & 0_3 & 0_3 & -R & 0_3 \\ (g)_{\times} & 0_3 & 0_3 & -(v)_{\times}R & -R \\ 0_3 & I_3 & 0_3 & -(p)_{\times}R & 0_3 \\ 0_3 & 0_3 & 0_3 & 0_3 & 0_3 \\ 0_3 & 0_3 & 0_3 & 0_3 & 0_3 \end{bmatrix}, Ad_{\chi} = \begin{bmatrix} R & 0_3 & 0_3 \\ (v)_{\times}R & R & 0_3 \\ (p)_{\times}R & 0_3 & R \end{bmatrix} \tag{10}$$

III. Kalman Filtering Algorithms on Lie Group for Sensor Fusion Problem

A. EKF Algorithm on Lie Group

State propagation

Theorem 2 in [12] ensured that state error η can be exactly reconstructed from (9). Mean state $\bar{\chi}_{k|k-1}$ and covariance matrix $P_{k|k-1}$ can be propagated using following formula,

$$\bar{\chi}_{k|k-1} = f_{u_k}\left(\bar{\chi}_{k-1|k-1}\right). \tag{11}$$

$$P_{k|k-1} = \Phi(t_k, t_{k-1})P_k\Phi(t_k, t_{k-1})^T + \bar{Q}_d \tag{12}$$

Measurement update

When new measurement data came, output innovation at time t_k will be updated as follows,

$$z_k = h\left(\exp(\xi_{\mathcal{L}})\circ\bar{\chi}\right) - h(\bar{\chi}) + V_k, V_k \sim \mathcal{N}\left(0_{6\times 1}, \Sigma^{leg}\right) \tag{13}$$

Analogous to (4), the output error with respect to $\xi_{\mathcal{L}}$ produces agumented Jacobian matrix H_k as follows,

$$H_k = \begin{bmatrix} \frac{1}{l_1}\left(a_1\times(Rb_1+p)\right)^T & 0_{1\times 3} & \frac{1}{l_1}(Rb_1+p-a_1)^T & 0_{1\times 3} & 0_{1\times 3} \\ \vdots & \vdots & \vdots & \vdots & \vdots \\ \frac{1}{l_6}\left(a_6\times(Rb_6+p)\right)^T & 0_{1\times 3} & \frac{1}{l_6}(Rb_6+p-a_6)^T & 0_{1\times 3} & 0_{1\times 3} \end{bmatrix}. \tag{14}$$

The Kalman gain K_k is calculated using the following two steps.

$$\begin{aligned} S_k &= H_k P_{k|k-1} H_k^T + R_k \\ K_k &= P_{k|k-1} H_k^T S_k^{-1} \end{aligned} \tag{15}$$

Finally, mean state and covariance matrix can be updated as follows.

$$\begin{aligned} \bar{\chi}_{k|k} &= \exp(K_k z_k)\circ\bar{\chi}_{k|k-1} \\ P_{k|k} &= \left[I - K_k H_k\right]P_{k|k-1} \end{aligned} \tag{16}$$

B. UKF Algorithm on Lie Group

The mean state to be estimated is propagated using deterministic IMU model.

$$\bar{\chi}_{k|k-1} = f_{u_k}\left(\bar{\chi}_{k-1|k-1}\right) \tag{17}$$

In order to determine propagated covariance $P_{k|k-1}$, we can rely on unscented transform to approximate distribution of augmented state $\chi_{\mathcal{L}}$ using selected sigma points in Lie algebra vector space. Then covariance $P_{k|k-1}$ can be determined as sum of weighted state error $\xi_{\mathcal{L}}^j$ as follows.

$$P_{k|k-1} = \sum_{j=1}^{q+k} W_j^c \log\left(\bar{\chi}_{\mathcal{L}}^{-1}\chi_{\mathcal{L}}^j\right)\log\left(\bar{\chi}_{\mathcal{L}}^{-1}\chi_{\mathcal{L}}^j\right)^T \tag{18}$$

Update

Unscented transform is again employed to pass each sigma point through inverse kinematic to output y_j.

$$y_j = h\left(\exp\left(\xi_{\mathcal{L}}^j\right)\circ\bar{\chi}_{k|k-1}\right) + v_j, j = 0,\cdots,2l \tag{19}$$

Thu we can approximate the posterior using mean value of length $\bar{y}$, covariance P_{yy} and cross-covariance $P_{\chi y}$ with reference to [9].

$$\begin{bmatrix} \bar{\xi}_{k|k} \\ * \end{bmatrix} = P_{\chi y}P_{yy}^{-1}\left(y_k - \bar{y}\right) \tag{20}$$

$$P_{k|k} = P_{k|k-1} - P_{\chi y}\left(P_{\chi y}P_{yy}^{-1}\right)^T \tag{21}$$

Finally, mean state can be updated in following formula.

$$\bar{\chi}_{k|k} = \exp\left(\bar{\xi}_{k|k}\right)\circ\bar{\chi}_{k|k-1}, \xi_{k|k} \sim \mathcal{N}\left(0, P_{k|k}\right) \tag{22}$$

C. Group Structure Influence Analysis

The simple form to combine SO(3), $\mathbb{R}^3$ and $\mathbb{R}^3\times\mathbb{R}^3$ is direct group, i.e. $\mathrm{SO}(3)\times\mathbb{R}^3\times\mathbb{R}^3\times\mathbb{R}^3$. However, as discussed in [14], semi-direct product showed computationall advantage in long-time numerical integration of kinematic reconstruction. The reason is that independent integration of angular and translation does not naturally produce a screw motion. From this point of view, we would expect improved filtering performance through appropriate choice of group structure.

For EKF-LG, it has been proved that deterministic IMU model using semi-direct product satisfies group affine property while other models using direct product don't. The highly nonlinearity of inverse kinematic of Stewart platform make it doesn't show the same invariance property as SLAM problem does.

For UKF, the retraction mapping $\mathcal{R}: G\times\mathbb{R}^n \to G$ is utilized to generate sigma poins. In TABLE I, we provide explicit formlation comparison on retraction mapping between direct product and semi-direct product. Considering the effect on EKF-LG, the choice of group structure would also have impacts on UKF performance.

TABLE I. Retraction Map between Direct Product and Semi-direct Product

Element	$SO(3)\ltimes\mathbb{R}^3$	$SO(3)\times\mathbb{R}^3$
R	$\exp(\xi_{\omega})R$	$\exp(\xi_{\omega})R$
v	$\exp(\xi_{\omega})v + \mathcal{J}(\xi_{\omega})\xi_v$	$v + \xi_v$
p	$\exp(\xi_{\omega})p + \mathcal{J}(\xi_{\omega})\xi_p$	$p + \xi_p$
b_a	$b_a + \xi_{b_a}$	$b_a + \xi_{b_a}$
b_g	$b_g + \xi_{b_g}$	$b_g + \xi_{b_g}$

IV. Evaluation of Different Kalman Filtering Algorithms

This section is devoted to verify performance of three kinds of filtering algorithms, UKF-LG, EKF-LG and UKF-Conv. A computer trajectory as well as simulated sensor measurement data are generated with reference to motion profile in paper [4]. In the motion profile, moving platform traces a circular with radius of 0.5m in horizontal plane with a period of 5s. A combined roll and pitch motion with angular velocity amplitude 10 deg/s and period 2.5s are accompanied with position change. All kinematic parameters of Stewart platform can be fund in [5].

TABLE II. Standard Deviation of Noise in IMU and Displacement Sensor

Parameters	Value	Parameters	Value
σ_x	$6.680\times10^{-4}\ m/s^2$	σ_{l_1}	$1.093\times10^{-5}\ m$
σ_y	$8.578\times10^{-4}\ m/s^2$	σ_{l_2}	$1.132\times10^{-5}\ m$
σ_z	$6.915\times10^{-4}\ m/s^2$	σ_{l_3}	$5.741\times10^{-6}\ m$
σ_p	$1.545\times10^{-4}\ m/s^2$	σ_{l_4}	$1.482\times10^{-5}\ m$
σ_q	$1.770\times10^{-4}\ m/s^2$	σ_{l_5}	$1.054\times10^{-5}\ m$
σ_r	$1.791\times10^{-4}\ m/s^2$	σ_{l_6}	$9.770\times10^{-6}\ m$

TABLE III. IMU Biases

Parameters		Value
b_a	λ_x	$4.898\times10^{-1}\ m/s^2$
	λ_y	$-9.023\times10^{-2}\ m/s^2$
	λ_z	$-1.894\times10^{-1}\ m/s^2$
b_g	λ_p	$-1.822\times10^{-2}\ rad/s$
	λ_q	$-5.067\times10^{-2}\ rad/s$
	λ_r	$-2.159\times10^{-2}\ rad/s$

A. Sensor Properties

In TABLE II, $\sigma_x,\sigma_y,\sigma_z$ and $\sigma_p,\sigma_q,\sigma_r$ denote standard deviation for accelerometer noise and gyro noise respectively, $\sigma_{l_1},\sigma_{l_2},\ldots,\sigma_{l_6}$ denote standard deviation for displacement sensor noise. IMU sensor is assumed to be polluted by time-invariant biases in TABLE III with gyro bias $b_g=(\lambda_x,\lambda_y,\lambda_z)$ and accelerometer bias $b_a=(\lambda_p,\lambda_q,\lambda_r)$. Fig. 2 shows selected measurement noise for IMU sensor and displacement sensors over a period of time.

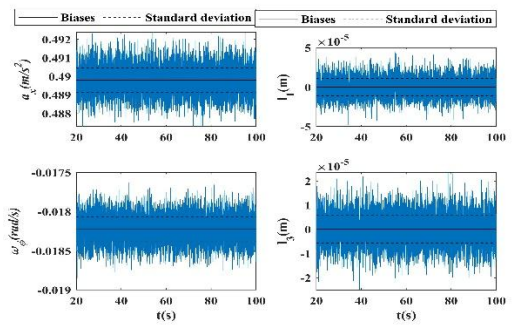

Fig. 2 IMU sensor noise and leg sensor noise

B. Initial Condition and Kalman Filtering Papameters

In initialization phase, we consider two cases of initial condition and filtering parameters. In the first case, initial kinematic state χ_0 is around true state while sensor biases are far away from true value. Thus initial covariance P_0 is relatively small. This case is mainly intended to test accuracy of these algorithms in a moderate fluctuation condition.

$$(\chi_0,b_0)=(R_0,v_0,p_0,(0,0,0),(0,0,0)) \tag{23}$$

$$P_0=diag\begin{pmatrix}(0.01\times\pi/180)^2,(0.01\times\pi/180)^2,(0.01\times\pi/180)^2,\\ 1\times10^{-8},1\times10^{-8},1\times10^{-8},1\times10^{-8},1\times10^{-8},1\times10^{-8},\\ 1\times10^{-12},1\times10^{-12},1\times10^{-12},1\times10^{-12},1\times10^{-12},1\times10^{-12}\end{pmatrix} \tag{24}$$

In second case, (χ_0,b_0) is assumed to be far away from true value and covariance P_0 is more or less enlarged with respect to motion envelope. Thus it is designed to check robustness of algorithms. The initial state χ_0 and P_0 are as follows.

$$(\chi_0,b_0)=(I_3,(0,0,0),(0,0,2.3893),(0,0,0),(0,0,0)) \tag{25}$$

$$P_0=diag\begin{pmatrix}(5\times\pi/180)^2,(5\times\pi/180)^2,(5\times\pi/180)^2,1,1,1,\\ 1,1,1,0.1^2,0.1^2,0.1^2,1,1,1\end{pmatrix} \tag{26}$$

In these two cases, noise covariance (Σ^a,Σ^g) and Σ^{leg} are both time-invariant and diagonal.

$$\begin{aligned}(\Sigma^a,\Sigma^g)&=1.1\times diag(\sigma_x^2,\sigma_y^2,\sigma_z^2,\sigma_p^2,\sigma_q^2,\sigma_r^2)\\ \Sigma^{leg}&=1.1\times diag(\sigma_{l_1}^2,\sigma_{l_2}^2,\sigma_{l_3}^2,\sigma_{l_4}^2,\sigma_{l_5}^2,\sigma_{l_6}^2)\end{aligned} \tag{27}$$

C. Results and Analysis

In order to evaluate filtering performance, RMSE for position is defined as square root of average of position error $\|\bar{p}-p\|_2^2$ while RMSE for orientation error is $\left\|\log_{SO(3)}(\bar{R}^TR)\right\|_2^2$ using logarithm map on SO(3).

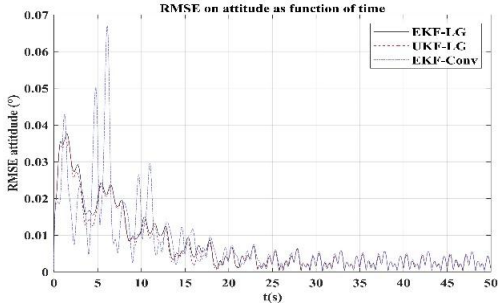

Fig. 3. RMSE attitude over time

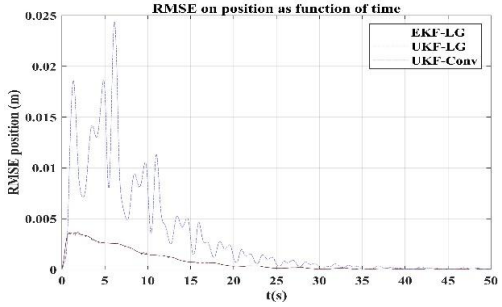

Fig. 4. RMSE potision over time

In the first case, Fig. 3 and Fig. 4 provide a performance comparison in position and orientation through RMSE error over time respectively. It reveals that all these filtering algorithms shows large estimation errors in the beginning when initial biases estimation are inaccurate. In transition stage, both UKF-LG and EKF-LG achieve similar faster convergent tendency than UKF-Conv. Especially for position error, UKF-Conv behaves with more violent oscillation than others. This is reasonable since orientation has no impact on translation under the framework of direct product.

Besides that, biases estimation also gain improvement as shown in Fig. 5 and Fig. 6.

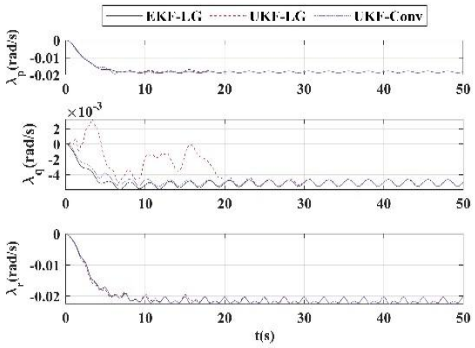

Fig. 5. Gyro bias estimation over time

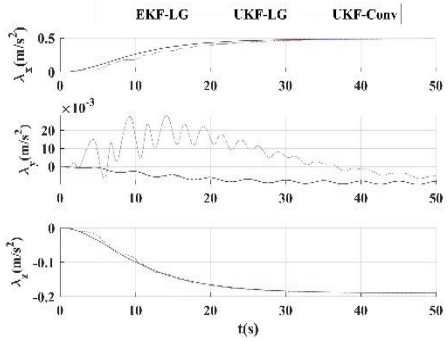

Fig. 6. Accelerometer bias estimation over time

As referred in Miletović's research [5], innovation sequences $\epsilon_k = \left(y_k - \overline{y}_{k|k-1}\right)$ at t_k tends to be a practical evaluation criteria. It is evident in Fig. 7 that UKF-LG outperforms UKF-Conv in length accuracy.

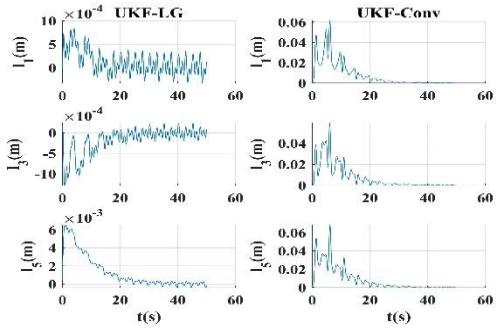

Fig. 7. Innovation sequences of leg (1,3,5) over time for UKF-LG and UKF-Conv algorithms

In the second case, TABLE IV shows averaged RMSE criteria comparison between these filtering algorithms. Results show that both position and orientation error are reduced to a larger scale using EKF-LG and UKF-LG than UKF-Conv algorithm.

TABLE IV. AVERAGED RMSE COMPARISON

Filtering algorithms	R(○)	P(m)
EKF-LG	0.0037	0.0004
UKF-LG	0.0040	0.0010
UKF-Conv	0.0441	0.0224

V. CONCLUSION

This paper discussed Kalman filtering on Lie group for sensor fusion problem of Stewart platform. After providing IMU model and inverse kinematic model, we build up EKF-LG and UKF-LG to trackle this problem. Evaluation of these two algorithms under simulated trajectory shows that both Lie group-based algorithms achieves almost the same better performance than UKF-Conv algorithm. This performance is attributed to semi-direct product which satisfies group affine property. A theoretical proof needs to be done in future research.

ACKNOWLEDGMENT

This work was jointly supported by Major Project of the New Generation of Artificial Intelligence, China(NO. 218AAA0102902).

REFERENCES

[1] S. K. Advani, R. J. Hosman, and M. Potter, "Objective motion fidelity qualification in flight training simulators," In AIAA Modeling and Simulation Technologies Conference and Exhibit, 2007. p. 6802.

[2] I. Davliakos and E. Papadopoulos, "Model-based control of a 6-dof electrohydraulic Stewart-Gough platform," Mechanism and Machine theory, vol. 43, no. 11, pp. 1385-1400, Dec. 2008.

[3] D. M. Pool, Q. P. Chu, M. M. Van Paassen and M. Mulder, "Optimal Reconstruction of Flight Simulator Motion Cues using Extended Kalman Filtering," In AIAA Modeling and Simulation Technologies Conference ans Exhibit, 2008. p. 6539.

[4] I. Miletovic, D. M. Pool, O. Stroosma, Q. P. Chu and M. M. Van Paassen, "Using iterated extended kalman filtering for estimation of a hexapod flight simulator motion state," In Proceedings of 11th PEGASUS-AIAA student conference, 2015.

[5] I. Miletovic, D. M. Pool, O. Stroosma, M. M. Van Paassen and Q. P. Chu, "Improved Stewart platform state estimation using inertial and actuator position measurements," Control Engineering Practice, vol. 62, pp. 102-115, 2017.

[6] T. D. Barfoot and P. T. Furgale, "Associating Uncertainty With Three-Dimensional Poses for Use in Estimation Problems," IEEE Transactions on Robotics, vol.33, no. 3, pp. 679-693, 2014.

[7] G. S. Chirikjian, "Stochastic models, information theory, ans Lie groups, volume 2: Analytic methods and modern applications," Springer Science & Business Media, 2010.

[8] G. Bourmaud, R. Megret, M. Arnaudon, A. Giremus, "Continuous-Discrete Extended Kalman Filter on Matrix Lie Groups using Concentrated Gaussian Distributions," Journal of Mathematical Imaging and Vision, Vol. 51, no. 1, pp. 209-228, 2015.

[9] S. Bonnabel, P. Martin, E. Salaün, "Invariant Extended Kalman Filter: theory and application to a velocity-aided attitude estimation problem," In Proceedings of the 48th IEEE Conference on Decision and Control (CDC) held jointly with 2009 20th Chinese Control Conference, pp. 1297-1304, 2009.

[10] M. Brossard, S. Bonnabel and A. Barrau, "Unscented Kalman Filter on Lie Groups for Visual Inertial Odometry," IEEE/RSJ International Conference on Intelligent Robots and Systems (IROS), pp. 649-655, 2018.

[11] A. Barrau and S. Bonnabel, "An EKF-SLAM algorithm with consistency properties," ArXiv preprint, arxiv:151006263, 2015.

[12] A. Barrau and S. Bonnabel, "The Invariant Extended Kalman Filter as a Stable Observer," IEEE Transactions on Automatic Control, vol. 62, no. 4, pp. 1797-1812, 2016.

[13] Y. Wang, "A direct numerical solution to forward kinematics of general Stewart-Gough platforms," Robotica, vol. 25, no. 1, pp.121-128, 2007.

[14] A. Muller and Z. Terze, "Geometric methods and formulations in computational multibody system dynamics," Acta mechanica, vol. 227, no. 12, pp. 3327-3350, 2016.

[15] A. Barrau and S. Bonnabel, "Invariant Kalman Filtering," Annual Review of Control, Robotics and Autonomous Systems, no. 1, pp. 237-257, 20